

## **Upgrade of JMA's Storm Surge Prediction for the WMO Storm Surge Watch Scheme (SSWS) in 2025**

**SUGANO Jumpei, KUBOKAWA Hiroyasu, FUKUURA Takashi and HASEGAWA Hiroshi**

Numerical Prediction Division, Japan Meteorological Agency

### **1. Introduction**

Since August 2022, the Japan Meteorological Agency (JMA) has operated the Asia-area storm surge ensemble prediction system (EPS) for the provision of real-time storm surge information to ESCAP/WMO Typhoon Committee Members within the framework of the WMO Storm Surge Watch Scheme (SSWS). For details of the system and related forecast products, see Hasegawa *et al.* (2023).

In January 2025, JMA upgraded the system to improve the accuracy of storm surge predictions. This report outlines the upgrade and associated verification results.

### **2. Upgrade**

#### **2.1 Astronomical tide database**

The Asia-area storm surge EPS utilizes harmonic constants based on a Finite Element Solution (FES) tidal model to calculate astronomical tides for locations where observation data are unavailable. For harmonic constants, the previous version (FES2014, Lyard *et al.* 2021) was replaced with the latest version (FES2022<sup>1</sup>).

#### **2.2 Unstructured grid**

A new unstructured grid was incorporated into the system for improved topography representation. As with the previous grid, JIGSAW (Engwirda 2017) was adopted as an unstructured mesh generation tool.

Figure 1 shows the previous (left) and new (right) grids for the area around Hong Kong Island. In the new grid, the representation of narrow straits and small islands is improved, allowing the system to operate storm surge predictions under more realistic conditions. There are also fewer grid points overall than in the previous grid, and computational consumption is reduced.

#### **2.3 Bottom friction scheme**

For the bottom friction coefficient  $c_b$ , Manning's drag coefficient formula (see, for example, Kerr *et al.* 2013) was adopted as

---

<sup>1</sup> The FES2022 Tide product was funded by CNES, produced by LEGOS, NOVELTIS and CLS and made freely available by AVISO". CNES, 2024. FES2022 (Finite Element Solution) Tidal model (Version 2024) [Data set]. CNES. <https://doi.org/10.24400/527896/A01-2024.004>

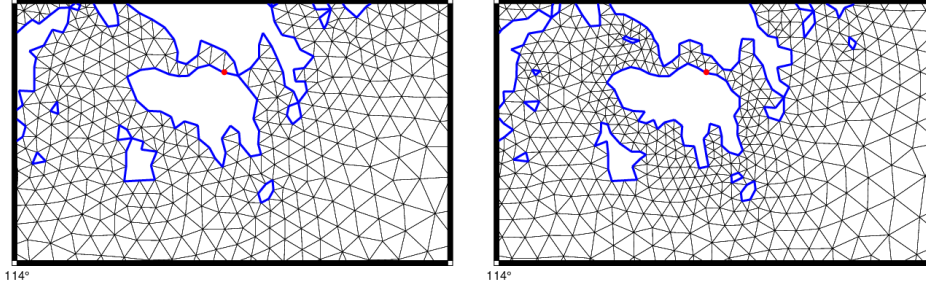


Figure 1 Comparison of previous (left) and new (right) unstructured grids around Hong Kong Island. Solid blue lines represent land-sea boundaries, and the red dot marks Quarry Bay.

$$c_b = \max\left(\frac{gn^2}{H^{1/3}}, c_{b,\min}\right) \quad (1)$$

to take into account depth dependence. Here,  $g$  is gravity acceleration,  $H$  is total depth,  $n$  is Manning's roughness and  $C_{b,\min}$  is a minimum coefficient value. In the system,  $n$  and  $C_{b,\min}$  are assumed to be 0.025 and  $2.6 \times 10^{-3}$ , respectively. Before modification,  $C_b$  was set as  $C_{b,\min}$ , i.e., a constant over the whole model domain. In Eq. (1), however,  $C_b$  exceeds  $C_{b,\min}$  when  $H$  is below around 8.5 m, and bottom friction stress is therefore strengthened.

## 2.4 Typhoon bogussing

The JMA Global Spectral Model (GSM) is used for atmospheric forcing in deterministic forecasting of the Asia-area storm surge EPS. Typhoon bogussing is also applied based on the official tropical cyclone (TC) forecast of JMA and implanted into GSM gridded data when any TC is present in the model domain within the forecast period (i.e., 132 hours).

However, the official TC forecast period is only up to 120 hours, which does not cover the forecast period of the system. Typhoon bogussing in the conventional scheme was abruptly removed from GSM gridded data at the end of the official TC forecast period, which caused a sharp change in atmospheric forcing and forecast values for areas around TCs. To address this, a new method was applied in which typhoon bogussing is gradually removed over a period of six hours after the end of the official TC forecast time.

## 3. Verification

### 3.1 Statistical verification of deterministic forecasting

To compare the performance of the previous (Cntl) and new (Test) systems, statistical verification of deterministic forecasting was conducted using storm surge observation data.

Figure 2 shows scatter diagrams of modeled storm surges against observation data from 10 SSWS stations (Table 1) where observation data are available on the University of Hawaii Sea Level Center (UHSLC) database website<sup>2</sup> and the Global Sea Level Observing System (GLOSS) website<sup>3</sup>. The statistical period is from April 2022 to December 2024, and cases of TCs are extracted. Figure 2 indicates generally

<sup>2</sup> <https://uhslc.soest.hawaii.edu/data/?fd>

<sup>3</sup> <https://www.ioc-sealevelmonitoring.org/index.php>

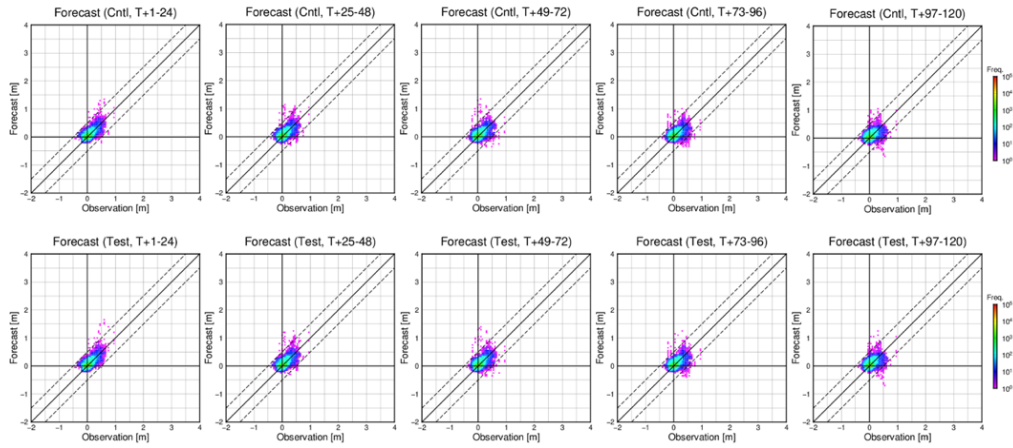


Figure 2 Scatter diagrams of modeled storm surges (vertical axis) against observation data (horizontal axis) in SSWS stations. The top and bottom panels are for the previous and new systems, respectively. All plots are three-hourly maximum values. Dashed lines denote the region within 0.5 m against observation.

Table 1 Stations used for verification

	Station	Abbreviation	Member	Data Source
1	Quarry Bay	QB	Hong Kong, China	UHSLC
2	Shek Pik	SP	Hong Kong, China	GLOSS
3	Langkawi	LK	Malaysia	UHSLC
4	Legaspi Port	LG	the Philippines	UHSLC
5	Manila South Harbor	ML	the Philippines	UHSLC
6	Subic Bay	SB	the Philippines	UHSLC
7	Quy Nhon	QN	Viet Nam	UHSLC
8	Vung Tau	VT	Viet Nam	UHSLC
9	Busan	BS	Republic of Korea	GLOSS
10	Apra Harbor	AP	U.S.A.	UHSLC

equivalent accuracy in both systems.

However, the results in Fig. 2 may not allow appropriate evaluation of model accuracy due to a lack of available observation data and the fact that no significant storm surges were observed at most stations during the statistical period. Hence, additional verification was conducted for tide stations in Japan, where observation data are sufficient for model accuracy evaluation (as per Hasegawa *et al.* 2023.)

Figure 3 displays scatter diagrams of modeled storm surges against observation data from around 200 stations in Japan (operated by JMA, the Ports and Harbours Bureau, the Japan Coast Guard and the Geospatial Information Authority of Japan). Other verification conditions are as per those for Fig. 2. The figure shows that overestimations tend to be improved in the new system throughout the forecast period, mainly due to the introduction of the new bottom friction scheme (Sec. 2.3).

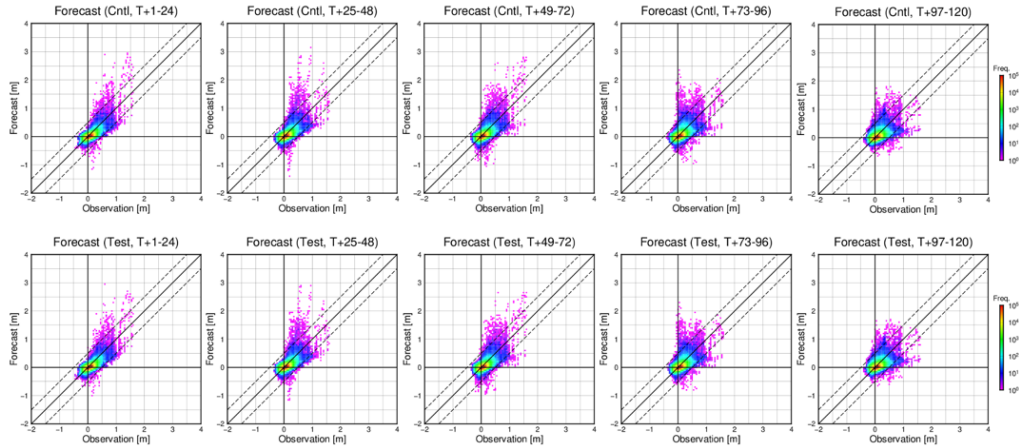


Figure 3 As per Fig. 2, but for stations in Japan.

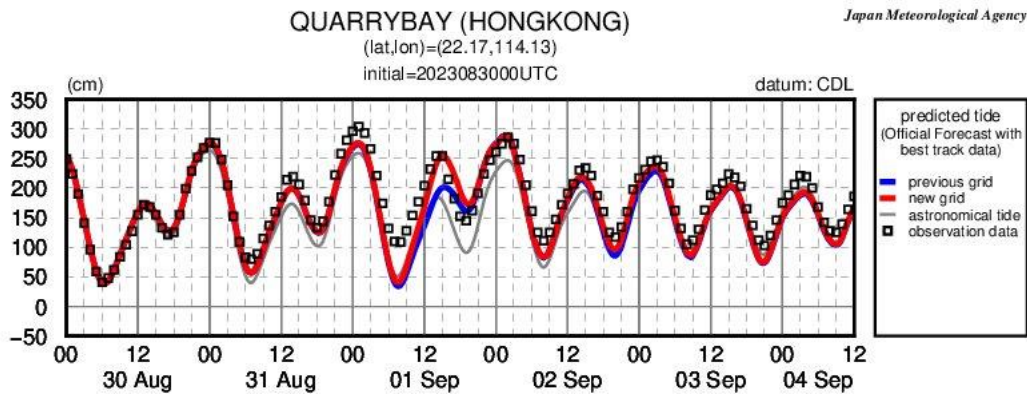


Figure 4 Time-series representation of storm tides (blue: previous grid; red: new grid) for Quarry Bay in Hong Kong based on best track calculation for 00 UTC on 30 August 2023. The grey line shows astronomical tides, and squares show hourly storm tide observation data.

### 3.2 Example: TY Saola (2309)

To evaluate the performance of the new unstructured grid, numerical simulations with the previous and new versions were conducted for TY Saola (2309). In both simulations, other upgrades were commonly applied and best track data were used to eliminate contamination from TC forecast errors (see also Annual Reports on Activities of the RSMC Tokyo – Typhoon Center 2023<sup>4</sup> for details of TY Saola (2309)).

Figure 4 shows a time-series representation of storm tides for Quarry Bay in Hong Kong at 00 UTC on 30 August 2023. Prediction with the new grid (red) competently reproduces the rise in storm tide around T+66, while that with the previous grid underestimates observation values. This indicates that the improved topographical representation enables storm surge prediction under more realistic conditions.

### 3.3 Example: TY Hinnamnor (2211)

In this section, numerical simulations for the conventional and new typhoon bogussing are compared

<sup>4</sup> <https://www.jma.go.jp/jma/jma-eng/jma-center/rsmc-hp-pub-eg/AnnualReport/2023/Text/Text2023.pdf>

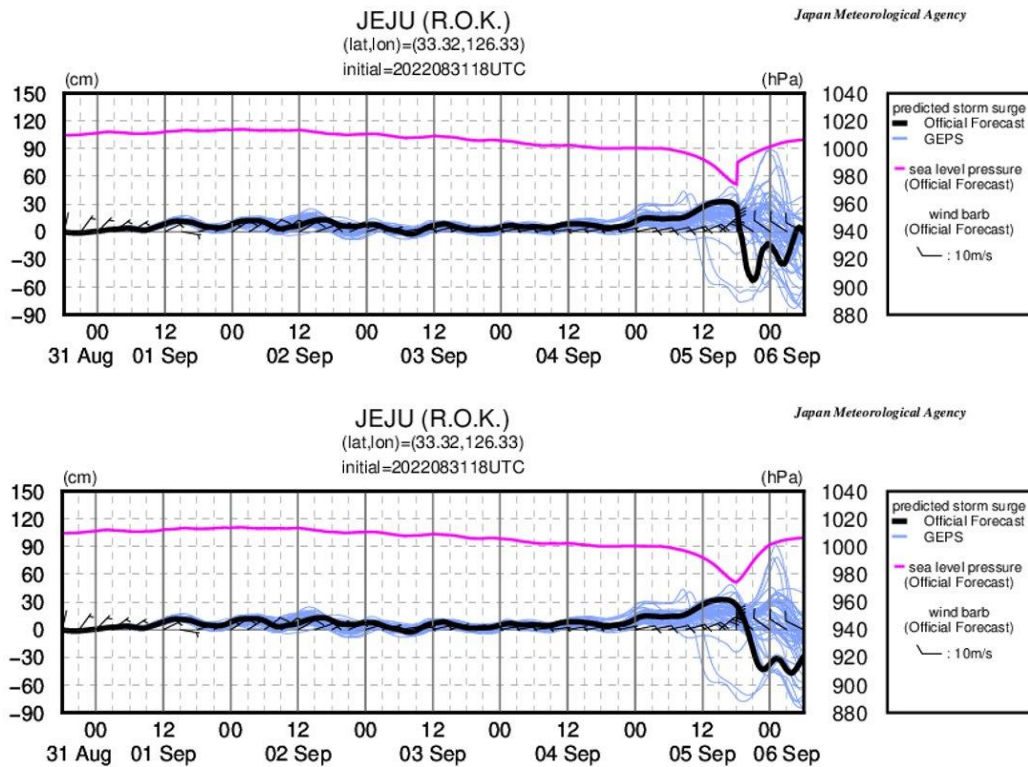


Figure 5 Time-series representation of storm surges and sea level pressure (top: previous typhoon bogussing; bottom: new one) for Jeju in the Republic of Korea at 18 UTC on 31 August 2022. The solid black line shows the storm surge of the official forecast, the thin blue lines show storm surges of the ensemble forecast, and the magenta line shows sea level pressure.

with TY Hinnamnor (2211) as a case study (see also Annual Reports on Activities of the RSMC Tokyo – Typhoon Center 2022<sup>5</sup> for details of TY Hinnamnor (2211)).

Figure 5 shows a time-series representation of storm surges and sea level pressure for Jeju in the Republic of Korea at 18 UTC on 31 August 2022. For the previous typhoon bogussing (top), a sharp pressure drop is seen just after T+120, where the official TC forecast is not available and typhoon bogussing is abruptly removed for the area around the TC. Conversely, smooth and natural temporal variations are seen with the new version (bottom) due to the gradual removal of typhoon bogussing from GSM gridded data.

<sup>5</sup> <https://www.jma.go.jp/jma/jma-eng/jma-center/rsmc-hp-pub-eg/AnnualReport/2022/Text/Text2022.pdf>

## References

- Hasegawa, H., J. Sugano, T. Fukuura, and M. Higaki, 2023: Upgrade of JMA's Storm Surge Prediction for WMO Storm Surge Watch Scheme (SSWS) in 2022. RSMC Tokyo-Typhoon Center Technical Review, **25**, 1-14, <https://www.jma.go.jp/jma/jma-eng/jma-center/rsmc-hp-pub-eg/techrev/text25-1.pdf>.
- Lyard, F. H., D. J. Allain, M. Cancet, L. Carrère, and N. Picot, 2021: FES2014 global ocean tide atlas: design and performance, *Ocean Sci.*, **17**, 615–649, <https://doi.org/10.5194/os-17-615-2021>.
- Engwirda, D., 2017: JIGSAW-GEO (1.0): locally orthogonal staggered unstructured grid generation for general circulation modelling on the sphere, *Geosci. Model Dev.*, **10**, 2117–2140, <https://doi.org/10.5194/gmd-10-2117-2017>.
- Kerr, P. C., R. C. Martyr, A. S. Donahue, M. E. Hope, J. J. Westerink, R. A. Luetlich Jr., A. B. Kennedy, J. C. Dietrich, C. Dawson, and H. J. Westerink, 2013: U.S. IOOS coastal and ocean modeling testbed: Evaluation of tide, wave, and hurricane surge response sensitivities to mesh resolution and friction in the Gulf of Mexico, *J. Geophys. Res. Oceans*, **118**, 4633–4661, <https://doi.org/10.1002/jgrc.20305>.